

# An Improved Scheme for a Robust High Resolution Measurement of Alveolar Oxygen Tension in Human Lungs

H. Hamedani<sup>1</sup>, K. Emami<sup>1</sup>, S. J. Kadlecek<sup>1</sup>, Y. Xu<sup>1</sup>, Y. Xin<sup>1</sup>, A. Barulic<sup>1</sup>, P. Mongkolwisetwara<sup>1</sup>, N. N. Kuzma<sup>1</sup>, P. Magnusson<sup>2</sup>, L. V. Søgaard<sup>2</sup>, S. Diaz<sup>3</sup>, P. Akeson<sup>2</sup>, G. W. Miller<sup>4</sup>, M. D. Rossman<sup>5</sup>, G. W. Miller<sup>6</sup>, and R. R. Rizi<sup>1</sup>

<sup>1</sup>Radiology, University of Pennsylvania, Philadelphia, PA, United States, <sup>2</sup>Danish Research Centre for Magnetic Resonance, Copenhagen University Hospital Hvidovre, Hvidovre, Denmark, <sup>3</sup>Department of Clinical Sciences, Malmö University Hospital, Malmö, Sweden, <sup>4</sup>Radiology, University of Virginia, Charlottesville, VA, United States, <sup>5</sup>Pulmonary, Allergy & Critical Care Division, University of Pennsylvania, Philadelphia, PA, United States, <sup>6</sup>Department of Radiology, University of Virginia School of Medicine, Charlottesville, VA

**INTRODUCTION:** Many pulmonary diseases stem from deficiencies of gas exchange in the lungs that can be parameterized by ventilation to perfusion ratio. It has been shown that the regional alveolar partial pressure of oxygen ( $P_{AO_2}$ ) in the lungs is closely related to the local ventilation-perfusion ratio. Over the years, a number of  $P_{AO_2}$  measurement techniques have been developed based on hyperpolarized (HP)  $^3\text{He}$  MRI with the goal of evaluating  $P_{AO_2}$  distribution in the lungs and quantifying the extent of pulmonary disease [1]. Most of them either suffer from low spatial resolution, require a long breath-hold or are limited to single slice acquisitions. To overcome these conflicting limitations, we present an improved scheme for  $P_{AO_2}$  imaging in humans over the entire lung, without substantially sacrificing the  $P_{AO_2}$  estimation accuracy.

**METHODS:** The relaxation rate ( $1/T_1$ ) of HP  $^3\text{He}$  gas increases in contact with oxygen molecules. This is the basis for almost all  $^3\text{He}$  techniques for local intrapulmonary  $P_{AO_2}$  measurement. A series of lung images are acquired during a breath-hold after inhalation of a mixture of  $^3\text{He}$ ,  $O_2$  and  $N_2$  gases, and the rate of HP  $^3\text{He}$  spin relaxation is computed based on this basic relationship:  $A_n(i, j, k) = A_0(i, j, k) \cos \alpha(i, j, k)^{nN_{PE}} \exp[-p_{O_2}(i, j, k) \cdot t_n(k)/\xi]$ , where  $A_0$  and  $A_n$  are the signal intensity of the

initial and  $n$ -th image respectively,  $(i, j, k)$  are the indices of a given voxel,  $\alpha$  is the local flip angle of the  $B_1$  field,  $N_{PE}$  is the number of phase encodes,  $\xi = 2.6$  [bar·s] is the oxygen-induced relaxation coefficient at body temperature, and  $t_n(k)$  is the start time of the  $n$ th acquisition of the  $k$ -th slice. This model incorporates the combined signal attenuation induced by both RF pulses and the interaction of  $^3\text{He}$  with  $O_2$  at an unknown  $P_{AO_2}$ , and therefore the unavoidable RF effect needs to be decoupled from that of  $O_2$ . A minimum of three images with *different* interscan time delays therefore are necessary for successful decoupling of the two effects (the decoupling is impossible for equal time delays regardless of the number of images). For a given total acquisition time (i.e. subject breath-hold time), the shorter time intervals correspond to more images which in turn require more RF pulses with a more pronounced RF-induced signal loss, whereas longer interscan time delays (i.e. fewer images) accentuate the effect of  $O_2$ -induced relaxation. Therefore the ideal timing strategy would utilize both short and long time intervals to maintain sensitivity to both effects.

**Figure 1(a)** shows the timing diagram of the more conventional *Single-Acquisition Sequence*. For a multi-slice measurement, a set of images is acquired sequentially from the first to last slice ( $N_S$ ) and repeated with a user-defined time delay except for the first two sets which are acquired with no delay (to satisfy the decoupling requirement and provide sensitivity to RF relaxation). In the proposed improved scheme shown in **Figure 1(b)**, two interleaved back-to-back images are acquired for each slice and this pattern is repeated as many times as the total breath-hold time allows. Separation of each pair of slices by the remaining slices in the lung volume eliminates the need for any additional time delays in-between the scans, thereby allowing to maximize the number imaged slices ( $z$  resolution) in contrast to the other approach. This technique also improves the RF- $O_2$  decoupling efficiency. Human experiments were performed under IRB-approved protocols for HP  $^3\text{He}$  MRI after obtaining subjects' informed written

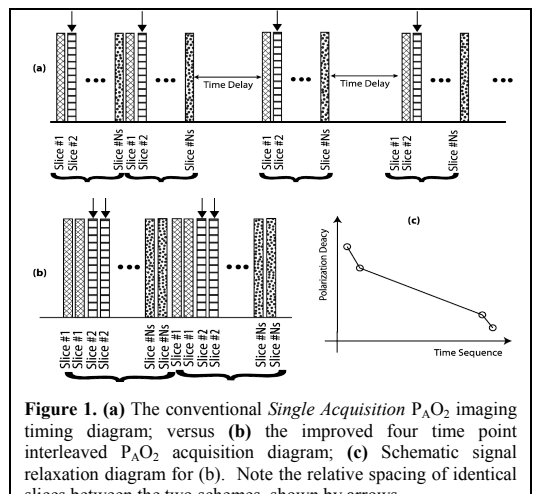


**Figure 1.** (a) The conventional *Single Acquisition*  $P_{AO_2}$  imaging timing diagram; versus (b) the improved four time point interleaved  $P_{AO_2}$  acquisition diagram; (c) Schematic signal relaxation diagram for (b). Note the relative spacing of identical slices between the two schemes, shown by arrows.

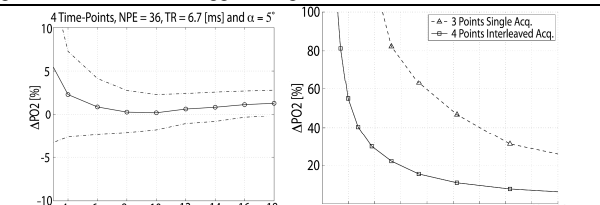


**Figure 2.** (a) Simulated relative decoupling error (solid line) and its variance in the presence of noise (dashed lines) as a function of time delay for the *Single Acquisition Sequence* with 4 time points; (b) Comparison of relative error between the two techniques in presence of noise.

consent prior to each experiment. This technique was tested on a healthy volunteer (57 yr, F) and compared for 3 vs. 4 sets of images during a 12-sec breath-hold covering the entire lung with 12 coronal slices.

Subject inhaled a mixture of  $^3\text{He}:N_2O_2$  ( $\text{FiO}_2 \approx 21\%$ ), with the total volume of 12%TLC. Images were acquired using a multi-slice gradient echo imaging pulse sequence with:  $TR/TE = 6.7/3.2\text{ms}$ ,  $FOV = 300 \times 400\text{mm}^2$ ,  $NS = 12$ ,  $ST = 13\text{mm}$ ,  $\alpha = 5^\circ$  and a matrix size =  $48 \times 36$  (L-R phase-encoding).

**RESULTS AND DISCUSSION:** The acquisition of 12 slices covering the entire lung took about 3 sec with the above parameters, thereby allowing us to image four sets of images (time points) in a 12-sec breath-hold. **Figure 2(a)** shows the simulated decoupling error (solid line) as a function of time delay in presence of noise for the single acquisition sequence. In order to limit the decoupling error with four time points, a time delay of 8 sec is required (minimum point), resulting in a total acquisition time of 28 sec which would be impractical in most cases, especially in patients with obstructive lung diseases. The interleaved acquisition scheme on the other hand can acquire the same number of time points in only 12 sec, making an efficient use of interscan time delay between the slices. **Figure 2(b)** shows the simulated relative error of  $P_{AO_2}$  estimation for the interleaved technique in presence of noise in comparison with the single acquisition technique, which corresponds to three time points with a time delay of 3 sec. For a fair comparison, the flip angle was increased for the three-time-point acquisition, in order to normalize the SNR of the last image in both sequences. A dramatic drop in the decoupling error was observed (by at least 20%-points, i.e. from 32% to 12%), while at low SNR values the interleaved technique shows up to a 80%-points improvement. The latter is a principal difference between a meaningful and a noise-dominated measurement. **Figure 3(a)** shows  $P_{AO_2}$  maps in the representative healthy volunteer, along with the frequency distribution histogram of  $P_{AO_2}$  over the entire lung shown in **Figure 3(b)**. The mean  $P_{AO_2}$  value of 103 mmHg is very close to the expected value of steady state  $P_{AO_2}$  in a healthy subject. Phantom studies (not shown) for a wide range of  $O_2$  concentrations confirmed marked improvement over prior techniques.

**CONCLUSION:** The proposed interleaved scheme provides a practical method for high-resolution imaging of  $P_{AO_2}$  distribution in human lungs with several demonstrated advantages over prior techniques. Shortening the breath-hold time requirement while maintaining high spatial resolution and estimation accuracy is a step towards making this diagnostically important pulmonary metric available to investigational studies in a more robust protocol.

**REFERENCES:** [1] Jalali, A. *et al.* Magn. Reson. Med. 51, 291 (2004).

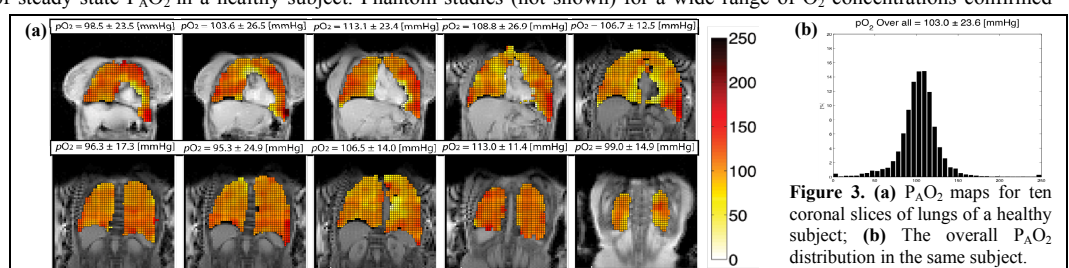


**Figure 3.** (a)  $P_{AO_2}$  maps for ten coronal slices of lungs of a healthy subject; (b) The overall  $P_{AO_2}$  distribution in the same subject.